Investigation Of The Mechanical Properties Of 3D Printed Compliant Mechanisms

Pham, Minh Tuan; Teo, Tat Joo; Yeo, Song Huat

2016

Pham, M. T., Teo, T. J., & Yeo, S. H. (2016). Investigation Of The Mechanical Properties Of 3D Printed Compliant Mechanisms. Proceedings of the 2nd International Conference on Progress in Additive Manufacturing (Pro-AM 2016), 109-115.

https://hdl.handle.net/10356/84630

INVESTIGATION OF THE MECHANICAL PROPERTIES OF 3D PRINTED COMPLIANT MECHANISMS

MINH TUAN PHAM
Singapore Centre for 3D Printing, School of Mechanical and Aerospace Engineering, Nanyang Technological University, Singapore 639798, Singapore
Mechatronics Group, Singapore Institute of Manufacturing Technology, Singapore 638075, Singapore

TAT JOO TEO
Mechatronics Group, Singapore Institute of Manufacturing Technology, Singapore 638075, Singapore

SONG HUAT YEO
School of Mechanical and Aerospace Engineering, Nanyang Technological University, Singapore 639798, Singapore

ABSTRACT: The compliant parallel mechanisms (CPM) used in precision positioners are commonly fabricated in parts by traditional manufacturing methods such as milling and wire-cut electrical discharge manufacturing (EDM). The performance of these positioners can therefore be significantly affected by assembling errors. This paper presents the investigation of the potential of 3D printing technology in fabricating precise-compliant devices through evaluating the performance of a 3D printed CPM. The design of a novel three degrees of freedom (DOF) CPM is first presented. The proposed CPM is monolithically fabricated by selective laser melting (SLM) technology, eliminating errors in the assembly process. Several experiments are carried out to evaluate the mechanical properties of the 3D printed CPM in terms of stiffness characteristics and dynamic response. The experimental performance of the 3D printed CPM is found to be within 12.5% of the results from simulation. The advantages as well as limitations of 3D printing technology in fabricating compliant devices are also discussed.

KEYWORDS: 3D printing, SLM, flexure, compliant mechanism, parallel mechanism

INTRODUCTION

Compliant mechanism has been a well-known device in precision motion systems like positioning stages. Based on the elastic deformation of materials, compliant mechanisms are able to produce highly repeatable motions that the conventional bearing based mechanisms fail to deliver. Hence, a number of devices in advanced robotic systems and micro/nano manufacturing/assembling fields are created depending on the good mechanical characteristics of compliant mechanisms such as monolithic structures, zero backlash, frictionless as well as maintenance-free (Howell et al. (2013)). Among two main forms of compliant mechanisms developed by serial and parallel configurations, compliant parallel mechanisms (CPMs) are preferred in precision motion systems due to the advantages of closed-form architecture such as less sensitive to external disturbances, higher payload but limited stroke. The development of CPMs is based on two domains, synthesis methodology and fabrication technology.

To satisfy the requirement of precision positioners, CPMs must provide desired degrees of freedom (DOF), large workspace, high stiffness ratios and fast dynamic response through the high

Proc. of the 2nd Intl. Conf. on Progress in Additive Manufacturing
Edited by Chee Kai Chua, Wai Yee Yeong, Ming Jen Tan, Erjia Liu and Shu Beng Tor

Published by Research Publishing, Singapore
ISSN: 2424-8967

frequency of the first resonant mode. A vast number of CPMs have been designed using various methods, from tasked-oriented method based on the construction of conventional rigid-mechanisms to optimization methods based on finite element analysis (Teo et al. (2014)). However, most of the existing designs are planar-motion CPMs, such as 2-DOF (X-Y) CPMs (Hui and Yangmin (2013); Li et al. (2013)) and 3-DOF (X-Y-θ_z) CPMs (Lum et al. (2014); Wang and Zhang (2008)). The number of multi-DOF spatial-motion CPMs has still been very limited.

Apart from synthesis methodology, fabrication technology determines the actual performance of CPMs. As the performance of CPMs much depends on the elastic deformation of complicated geometry, e.g. small notches and thin beams, the fabrication process must provide high accuracy and is able to fabricate complex structures. The most popular methods to fabricate compliant mechanisms are by milling and wire-cut electrical discharge machining (EDM). Even though the high accuracy can be obtained, only planar-metal mechanisms can be fabricated monolithically by wire-cut EDM. On the other hand, milling technology can fabricate complex structures but the accuracy is affected by the effects of cutting forces. Because of the limitations of current fabrication methods, complex designs of CPMs must be separated into many parts to be fabricated and then assembled. As a result, errors in the fabricating and assembling processes may reduce the performance of CPMs. Therefore, the designs of existing CPMs, especially synthesized by optimization methods, are always constrained by the manufacturing technology.

In recent years, 3D printing technology is fast developing and gaining attention in many industrial fields, it can be considered as a good solution for fabricating complex designs based on additive manufacturing strategy. By applying 3D printing to fabricate CPMs, the assembling errors can be completely eliminated and the complex structures will not be a constraint. However, the number of CPMs fabricated by 3D printing technology is still very limited and their behaviors of have not been reported.

To address the existing problem in synthesizing and fabricating CPMs, this paper presents a new design of 3-DOF spatial-motion (θ_x-θ_y-Z) CPM and selective laser melting (SLM), a popular powder-based 3D printing method, is applied to fabricate the synthesized CPM monolithically. The performance of the 3D printed prototype will be experimentally evaluated to explore the advantages as well as disadvantages of using 3D printing technology for precise-compliant devices through the behaviors of the 3D printed CPM.

SYNTHESIS PROCESS OF THE 3-DOF (θ_x-θ_y-Z) CPM

In this section, a new design of 3-DOF (θ_x-θ_y-Z) CPM is synthesized to satisfy both static and dynamic requirement for developing positioning stage. Subsequently, SLM is used to fabricate the synthesized CPM to address the complex structure as well as reduce the manufacturing time and cost. AlSi10Mg is the selected material, its mechanical properties are listed in Table 1.

Table 1. Mechanical properties of AlSi10Mg material

Young modulus (GPa)	In horizontal direction (XY)	75
	In vertical direction (Z)	70
Yield strength (MPa)	In horizontal direction (XY)	270
	In vertical direction (Z)	240
Poisson ratio		0.33
Density (g/cm^3)		2.67

A CPM consists of an end effector that is connected by several compliant limbs as frictionless support bearings. The 3-limb rotational-symmetrical configuration as shown in Figure 1(a) is used as the design domain in this work. The multi-DOF spatial-motion CPM is synthesized by employing the high flexibility of the curved-twisted (C-T) beams, which are the basic design modules of each compliant limb as illustrated in Figures 1(b) and (c). The design space of each compliant limb is $50 \times 50 \times 50$ mm^3 to fit the building area of 3D printing machine.

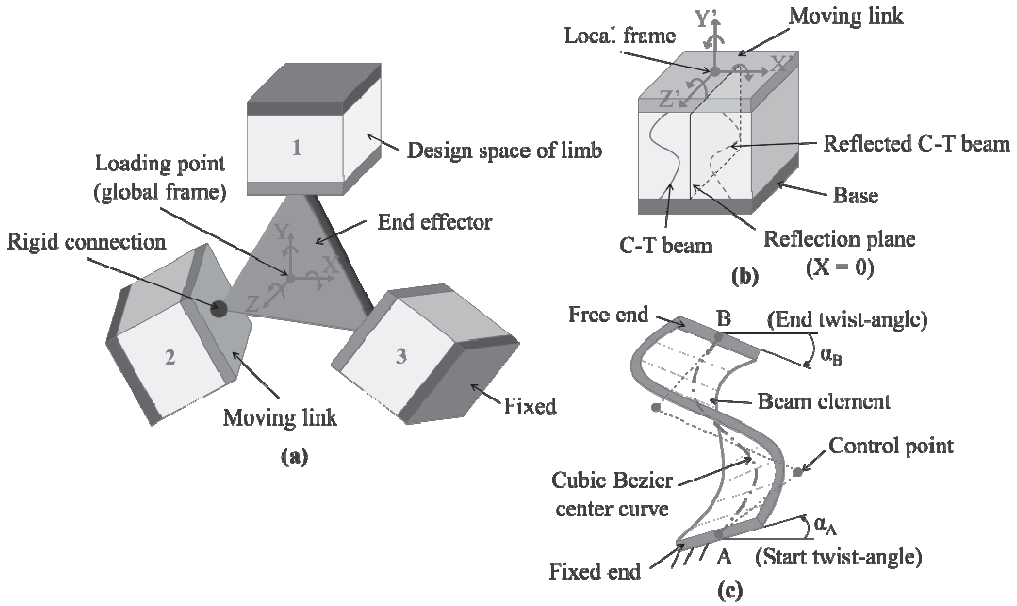

Figure 1. General models used in synthesis process (a) 3-limb configuration CPM (b) structure of a compliant limb and (c) construction of a C-T beam

The synthesis process is separated into two steps, stiffness and dynamic optimization. The purpose of the stiffness optimization process is to find out the best geometry of the C-T beams that provide the desired DOF, the largest workspace and the highest stiffness ratios. The dynamic optimization process is then carried out to determine the shape of the C-T beams as well as defining the material distribution within the CPM so as to achieve the targeted first resonant frequency.

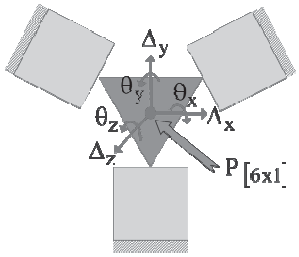

Figure 2. Displacements of the CPM under a general load at the end effector

The CPM is considered under effect of a general load vector, $P = \{F_x, F_y, F_z, M_x, M_y, M_z\}$, that contains three forces F_x, F_y, F_z components along the X, Y and Z axes respectively, and three

moments M_x, M_y, M_z components about the X, Y and Z axes respectively. The loading point is at the center of the end effector as illustrated in Figure 1. The corresponding displacements generated by P are represented by the displacement vector, $U = \{\Delta_x, \Delta_y, \Delta_z, \theta_x, \theta_y, \theta_z\}$, as shown in Figure 2.

The proposed C-T beams are discretized into many segments using beam elements as illustrated in Figure 1(c) and finite element analysis (FEA) is employed to analyze the behavior of the CPM. The fitness function of the stiffness optimization process, f, as written in Eq. (1) is derived to maximize the workspace and the stiffness ratios of the CPM by minimizing the product of the works done ratios.

$$min\ f = \left(\frac{W_{\theta_x}}{W_{\Delta_x}} \cdot \frac{W_{\theta_x}}{W_{\Delta_y}} \cdot \frac{W_{\theta_x}}{W_{\theta_z}}\right) \cdot \left(\frac{W_{\theta_y}}{W_{\Delta_x}} \cdot \frac{W_{\theta_y}}{W_{\Delta_y}} \cdot \frac{W_{\theta_y}}{W_{\theta_z}}\right) \cdot \left(\frac{W_{\Delta_z}}{W_{\Delta_x}} \cdot \frac{W_{\Delta_z}}{W_{\Delta_y}} \cdot \frac{W_{\Delta_z}}{W_{\theta_z}}\right) = \left(\frac{W_{\theta_x}}{W_{\Delta_x}} \cdot \frac{W_{\theta_y}}{W_{\Delta_y}} \cdot \frac{W_{\Delta_z}}{W_{\theta_z}}\right)^3 \quad (1)$$

In Eq. (1), W_i is the work done of the i DOF ($i \in U$) generated by the i^{th} components of vectors P and U, given as

$$W_i = P_i \cdot U_i \quad and \quad U_i = C_i \cdot P_i \quad (2)$$

Where C_i is the compliance of the CPM on the i DOF.

Genetic Algorithm (GA) is used to solve the optimization problem and the 3D CAD model of the stiffness optimization result is shown in Figure 3(a). To obtain the requirement of dynamic response, the dynamic optimization must be carried out to ensure the first resonant frequency of the CPM reach the desired value. The fitness function of the dynamic optimization process is expressed by two equations as written in Eq. (3). The first resonant frequency, F_1, of the CPM is guaranteed to match the desired value, F_d, by the first equation. The stiffness properties of the CPM are maintained as well as possible by the second equation. The 3D CAD model of the final CPM is shown in Figure 3(b) and the synthesizing results of the CPM are presented in Table 2.

$$\begin{cases} min\left(\left|F_1 - F_d\right|\right) \\ min\left(f\right) \end{cases} \quad (3)$$

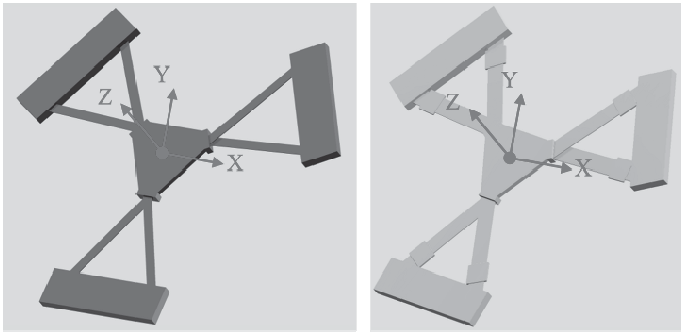

(a) (b)

Figure 3. The CPM after (a) stiffness optimization process and (b) dynamic optimization process

EXPERIMENTS AND RESULTS

The prototype of the synthesized CPM in Figure 3(b) is built by SLM to evaluate the abilities of 3D printing technology in fabricating precise-compliant devices. The CPM is printed with the minimum thickness of 0.6 mm. The details of the 3D printed CPM are shown in Figure 4. Note that the end effector was made bigger to accommodate for external actuators and its thickness was reduced while some supporting ribs were added to maintain the original mass and stiffness. Even though the overall shape of the prototype is fine but several issues exist when using 3D printing to fabricate the synthesized CPM. The quality of surfaces is bad and varies through the prototype. The warpage due to thermal effect is significant and badly affects to the structure, especially to the thin beams. In addition, the accuracy is not unique through the entire CPM. Although the mentioned issues could reduce the performance of the 3D printed CPM, the monolithic structure is the major advantage since eliminating all assembling errors.

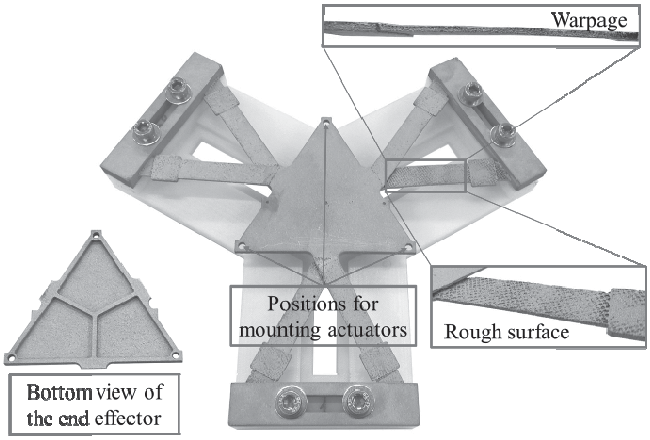

Figure 4. SLM prototype of the synthesized CPM

The experimental setup for evaluating the compliance along the Z axis is shown in Figure 5(a). A micrometer with 10 μm resolution was used to provide input displacement along the Z axis while a 6-axis force/torque (F/T) sensor was employed to measure the actuating force concurrently. In addition, a rigid rod with a sharp tip was used to apply the force at the end effector's center.

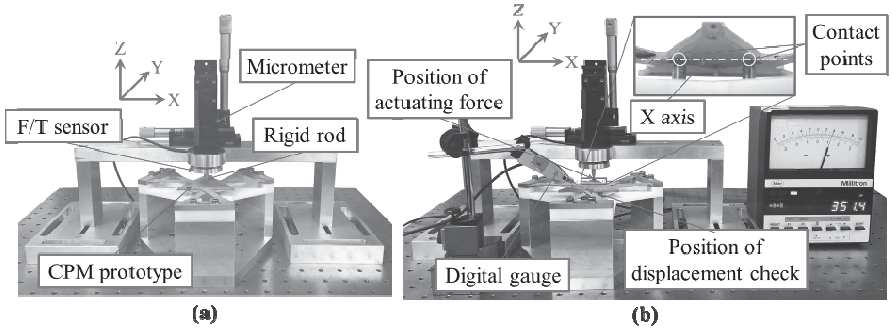

Figure 5. Experimental setup for evaluating the compliance (a) along the Z axis and (b) about the X (or Y) axis

To evaluate the compliance about the X axis, a two-point support was placed below the end effector as shown in Figure 5(b) to constrain the motion along the Z axis so that the end effector can deliver pure rotational motion about the X axis. The similar concept was adopted when evaluating the compliance about the Y axis. The actuating force and displacement were applied and measured at one point respectively to calculate the bending moment as well as the rotation angle. To ensure a pure rotational motion was produced for each measurement, a digital gauge was used to measure the displacement at the opposite position, making sure it was similar to the input displacement.

The experimental investigation was conducted by measuring the actuating force at six different positions and conducted over five times. Figure 6 presents the experimental and predicted compliance of the CPM.

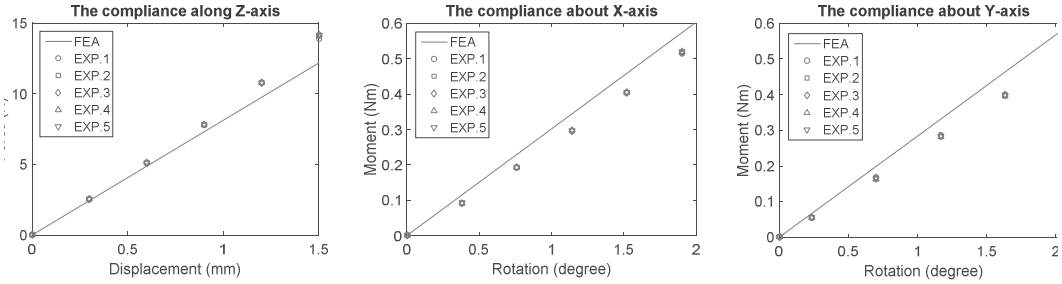

Figure 6. Experimental compliance of the 3D printed CPM

The experimental setup for measuring the frequency response of the CPM is shown in Figure 7(a). Because FEA result showed that the first resonant mode is along Z direction, an accelerometer was used to measure the acceleration of the end effector along the Z axis, which was generated by an input force applied in the same direction of the impact hammer. Figure 7(b) shows the dynamic response of the CPM obtained from the output data of the modal analysis equipment.

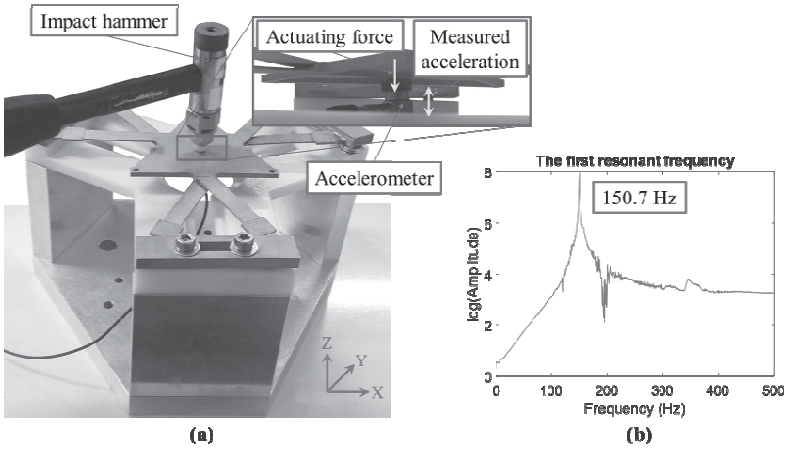

Figure 7. (a) Experimental setup and (b) result of the dynamic response

The workspace of the 3D printed CPM is $4^o \times 4^o \times 3$mm based on the FEA result and it was also demonstrated by the experiments. In addition, the CPM fabricated by SLM is able to provide highly repeatable manipulations with very small positioning errors as seen in Figure 6. To evaluate the performance of the 3D printed CPM, the comparison between the FEA and experimental results are summarized in Table 2.

Table 2. Comparison between the FEA and experimental results of the 3D printed CPM

Property	*FEA*	*Experiments*	*Deviation*
Compliance along Z axis (m/N)	1.23E–4	—–	~ 7.0%
Compliance about X axis (rad/Nm)	5.76E–2	—–	~ 11.8%
Compliance about Y axis (rad/Nm)	6.21E–2	—–	~12.5%
The first resonant frequency (Hz)	142	150.7	6.1%

It is seen that the experimental results well match with the FEA, the maximum deviation is less than 13%. Although the manufacturing accuracy of SLM is not good, thanks to the monolithic structure for eliminating the assembling errors and enhancing the performance of the CPM.

CONCLUSION

This paper proposed a new design of a 3-DOF spatial-motion (θ_x-θ_y-Z) CPM with optimized stiffness and dynamic properties. The synthesis process was briefly discussed and the prototype of the synthesized CPM was fabricated by SLM with AlSi10Mg material. Several experiments were carried out to evaluate the properties of using 3D printing technology to fabricate precision motion systems like CPM. Even though the quality of 3D printed CPM is not so good due to the warpage and rough surfaces, the performance of the 3D printed CPM is fine since the maximum deviation between the simulated and experimental results are about 12.5%. The results demonstrate 3D printing technology can be applied to fabricate precise-compliant devices and this is the opportunity for developing complex designs of multi-DOF CPMs.

ACKNOWLEDGEMENT

The first author would like to acknowledge the funding of the National Research Foundation.

REFERENCES

Howell, L.L., Magleby, S.P., Olsen, B.M., 2013. Handbook of compliant mechanisms. John Wiley & Sons.

Hui, T., Yangmin, L., 2013. Design, Analysis, and Test of a Novel 2-DOF Nanopositioning System Driven by Dual Mode. IEEE Transactions on Robotics 29, 650-662.

Li, X., Tian, Y., Qin, Y., Wang, F., Gao, W., Zhang, D., Eichhorn, V., Fatikow, S., 2013. Design, Identification and Control of a 2-Degree of Freedom Flexure-Based Mechanism for Micro/Nano Manipulation. Nanoscience and Nanotechnology Letters 5, 960-967.

Lum, G.Z., Teo, T.J., Yang, G., Yeo, S.H., Sitti, M., 2014. Integrating mechanism synthesis and topological optimization technique for stiffness-oriented design of a three degrees-of-freedom flexure-based parallel mechanism. Precision Engineering 39, 125-133.

Teo, T., Yang, G., Chen, I.M., 2014. Compliant Manipulators, in: Nee, A.Y.C. (Ed.), Handbook of Manufacturing Engineering and Technology. Springer London, pp. 2229-2300.

Wang, H., Zhang, X., 2008. Input coupling analysis and optimal design of a 3-DOF compliant micro-positioning stage. Mechanism and Machine Theory 43, 400-410.